UNIVERSIDAD MICHOACANA DE SAN NICOLAS DE HIDALGO

Foro de Ingeniería e Investigación en Materiales

Cuerpo Académico Consolidado CA-105: Ingeniería y Tecnología de Metales, Cerámicos y Aleaciones

INSTITUTO DE INVESTIGACIÓN EN METALURGIA Y MATERIALES

EFFECT OF WC NANOPARTICLES ON THE COBALT BASED OVERLAY DEPOSITED ON H13 STEEL BY PLASMA TRANSFERRED ARC (PTA)

A.V. ZAMORA-LÓPEZ[1]*, F.J. GARCÍA-VÁZQUEZ[2], H.M. HERNÁNDEZ-GARCÍA[1], A. ARIZMENDI-MORQUECHO[3], J. ACEVEDO-DÁVILA[1]

[1] Corporación Mexicana de Investigación en Materiales (COMIMSA), Calle ciencia y tecnología No. 790, Col. Saltillo 400, Saltillo, Coahuila, C.P. 25290.
[2] Facultad de ingeniería (UAdeC), Km.13 Ciudad Universitaria, Lat. Bulevar Fundadores, Zona Centro, Arteaga, Coahuila, C.P. 25350.
[3] Centro de Investigación en Materiales Avanzados (CIMAV), Alianza Nte. 202 Parque PIIT, Apodaca, N.L., C.P. 66600 A.P. 43.

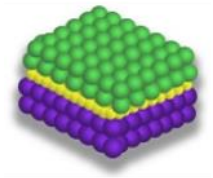

FORO DE INGENIERÍA E INVESTIGACIÓN EN MATERIALES. **VOL. 13** (2016) 1-8
Editores: E.A. Aguilar, E. Bedolla, C.A. León

Morelia, MÉXICO.
ISSN 2448-6892

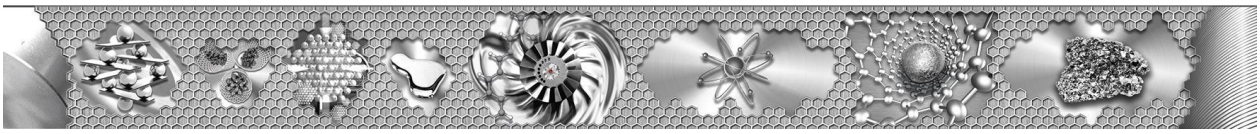

* A.V. Zamora-López (✉)
email: alberto.vzl@gmail.com

EFFECT OF WC NANOPARTICLES ON THE COBALT BASED OVERLAY DEPOSITED ON H13 STEEL BY PLASMA TRANSFERRED ARC (PTA)

A.V. ZAMORA-LÓPEZ[1]*, F.J. GARCÍA-VÁZQUEZ[2], H.M. HERNÁNDEZ-GARCÍA[1], A. ARIZMENDI-MORQUECHO[3], J. ACEVEDO-DÁVILA[1]

[1] Corporación Mexicana de Investigación en Materiales (COMIMSA), Calle ciencia y tecnología No. 790, Col. Saltillo 400, Saltillo, Coahuila, C.P. 25290.
[2] Facultad de ingeniería (UAdeC), Km.13 Ciudad Universitaria, Lat. Bulevar Fundadores, Zona Centro, Arteaga, Coahuila, C.P. 25350.
[3] Centro de Investigación en Materiales Avanzados (CIMAV), Alianza Nte. 202 Parque PIIT, Apodaca, N.L., C.P. 66600 A.P. 43.

Introduction

Hardfacing is one of the most attractive surface engineering methods employed to enhance the wear and corrosion–oxidation resistance of surfaces [1]. For this purpose plasma transferred arc (PTA) hardfacing process is a suitable alternative compared with welding arc process as SMAW, GMAW and GTAW, in terms of its high deposition rate, lower heat input, excellent arc stability and most importantly, the wide amount of filler metals [2,3].

Cobalt-based alloys have extensive use in wear related engineering applications for well over 50 years because of their inherent high-strength, corrosion resistance and ability to retain hardness at elevated temperatures [4]. Several properties of these alloys arise from the crystallographic nature of cobalt, the solid-solution-strengthening effects of chromium, tungsten and molybdenum, the formation of metal carbides, and the corrosion resistance imparted by chromium [5-7]. Cobalt presents an hexagonal crystal structure (hcp) at room temperature, transforming to cubic form (fcc) at higher temperatures (above 400 °C). The stacking fault energy of both allotropes is low, which offers better response to stress [7]. Chromium also provides oxidation and corrosion resistance by forming an adherent oxide film at high temperatures while refractory metals such as molybdenum and tungsten contribute to the strength via precipitation hardening by forming MC and M_6C carbides and intermetallic phases such as Co_3 (Mo, W) [8].

Stellite alloys are a group of cobalt-based superalloys with the main constituents belonging to the quaternary systems Co–Cr–W–C or Co–Cr–Mo–C. These alloys are generally strengthened by the precipitation of carbides in their cobalt matrix. The most important differences among Stellite alloys are their carbon and tungsten contents, which affect the type and amount of carbide formation in their microstructures [9]. The aim of this work is to study the effect of WC NPs on

ISSN 2448-6892

the microstructure, hardness and abrasive sliding wear behavior in cobalt-based Stellite 12 deposited overlays. This alloy was added with 0.5 and 2 wt% WC NPs and deposited by Plasma Transferred Arc (PTA) on heat treated hot work tool steel.

Methodology

Preparation of nanostructured filler metal

For the impregnation of the Stellite 12 filler metal (150/45 µm, Kennametal) with WC NPs (80 nm, Skyspring Nanomaterials). Separately, the WC NPs in 250 ml of ethanol were dispersed and sonicated for 1 h. Subsequently, the filler metal was placed into the dispersed WC NPs and sonicated for 3 h. This sonication process promotes the incorporation of WC NPs into the secondary interdendritic branches of the filler metals. This process was carried out with 0.5 and 2 wt% of WC NPs on the Stellite 12 filler metal, respectively. These samples are labeled as Stellite 12 without NPs (ST1), Stellite 12 with 0.5 and 2 wt% of WC NPs (ST2) and (ST3), respectively.

Alloy deposition and weld metal characterization

Hot work tool steel plates (H13) were thermally treated before the welding process. This thermal treatment was carried out with a preheating at 845 °C for 1 h and followed with an austenized at 1020 °C for 45 min and, quenched in circulating air. After that, the samples were tempered twice at 595 °C for 2 h in order to reach a microhardness of 499 HV to have the best microstructural condition. The Stellite 12 without and with WC NPs were deposited on 25 mm thick AISI H13 heat-treated hot work tool steel, using the PTA overlaying process shown in Fig. 1. The PTA equipment consists of two power sources, one the Fronius Transtig 1700 to the pilot arc and the Fronius Transtig 4000 to the plasma arc. The parameters used in this study are listed in Fig. 1. The metal powders injected from a powder feeder are melted inside the plasma arc flame and the melted metal powders thus obtained are deposited on the substrate.

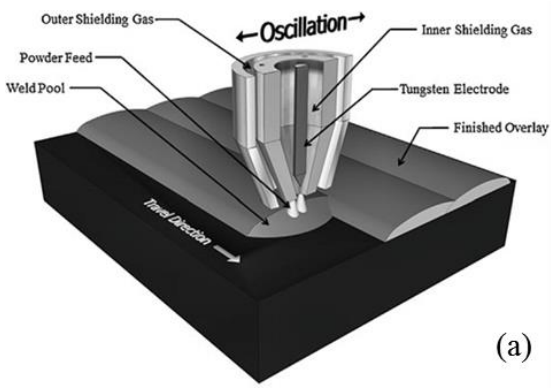

(b)

Parameters	
Main arc current (A)	165
Travel speed rate (cm/min)	17
Powder feed rate (g/min)	20
Torch gap (mm)	10
Shielding gas - Ar (lpm)	12
Plasma gas - Ar (lpm)	5
Carrier gas - Ar (lpm)	5
Preheating (°C)	350

Fig. 1. Schematic of the PTAW process [10] (a). PTA welding parameters (b).

ISSN 2448-6892

The coated samples were polished mechanically and chemically etched by submerged in a solution of H_3PO_4(10%) + H_2SO_4(50%) + HNO_3(40%) in order to reveal their microstructures. These samples were examined at high amplifications using Nikon SMZ745T stereo, Nikon Eclipse MA200 optical and a JEOL JSM-6490LV model scanning electron microscope (SEM) fitted with an Oxford Instruments INCA x-sight model energy dispersive X-ray analyzer (EDS). The microhardness of the samples were measured in Vickers across the overlay, the heat affected zone and the unaffected substrate with a Wilson Tukon 2500 automated Knoop/ Vickers microhardness tester, with a load of 0.5 kg (HV0.5).

Measurements of microhardness and wear resistance on the overlay.

The tribological behavior of overlays was investigated under sliding wear using a CSM pin-on-disk tribometer, according to ASTM: G99-05. During the test, the specimen was spinning at a linear speed of 10 cm/s over a distance of 1000 m. The pin was placed at a distance of 6 mm away from the rotation center on the specimen surface under a compressive force of 5N without lubrication. As a result of friction/wear, a circular wear track was created on the specimen surface. The pin was a sapphire ball of 6 mm diameter. The wear loss was evaluated by calculating the volume of the wear track after the specimen surface was worn for 2.78 h. The friction was recorded automatically throughout the test with the aid of a linear variable displacement transducer and the coefficient of friction was calculated in real time with the built-in software.

Results and discussion

Alloy deposition and weld metal characterization

The chemical composition of H13 steel substrate and filler metal without and with WC NPs is presented in the Table 1. A characteristic of the steel substrate is the contents of C, Mo, Cr, Nb and V, which influence in the precipitation of the strengthening carbides that increase the mechanical properties at high temperature. In the case of filler metals the Co improves the corrosion resistance and ability to retain hardness at high temperatures and precipitate as Co_3Ti which is a coherent phase with the matrix. In addition, reports in the literature [11-13] suggest that cooling of the PTA deposited Stellite 12 overlay from the liquid state involves a primary Co-rich solid solution dendritic matrix and the remaining liquid eventually solidifies by a eutectic reaction into a lamellar mixture of a Co-rich solid solution phase with Cr-rich carbides [14]. The W and C as WC for ST2 and ST3 can act as reinforcing particular in the overlays by the

ISSN 2448-6892

formation of rings for dislocations with the particles as has been presented in the work of Orowan [15], given as:

$$\tau_o = \frac{Gb}{\lambda} \qquad (1)$$

where τ_o, shear stress (MPa); G, shear module (GPa); b, Burger´s vector (nm) and λ, interparticle spacing (nm).

Table 1. Chemical composition (wt%) of hot work tool steel substrate, pure filler metal and combinations with WC NPs.

Material	Co	Cr	W	C	Ni	Mo	Fe	Si	S	Mn	P	Cu	V	Nb	Ti	WC NPs
AISI H13	-	4.15	0.051	0.37	0.11	1.31	Bal.	1.18	0.0003	0.29	0.026	0.072	0.948	0.011	0.008	-
ST1	Bal.	30.00	8.50	1.45	2.00	0.90	1.00	1.00	-	-	-	-	-	-	-	-
ST2	Bal.	29.85	8.46	1.44	1.99	0.90	1.00	1.00	-	-	-	-	-	-	-	0.5
ST3	Bal.	29.40	8.33	1.42	1.96	0.88	0.98	0.98	-	-	-	-	-	-	-	2.0

Fig. 2 shows, at high amplifications, microstructures of the cross-section on the examined overlays of ST1, ST2 and ST3 overlay, respectively. As can be appreciated in the Fig. 2, the overlays have a dendritic microstructure with phases dispersed among the interdendritic regions in the cobalt-rich matrix. Because of that an enriched liquid fraction of eutectic is trapped during the solidification. The literature suggests that a lamellar eutectic mixture of fcc phase and M_7C_3 eutectic carbides is formed by a eutectic reaction into an inter-dendritic region from the remaining liquid [16].

Comparatively, the impregnated Stellite 12 with WC NPs allows a slight refinement of the microstructure thereby gives rise the reduction of inter-dendritic region as shown in the Fig. 2 (b) and (c). It is postulated that the WC NPs can increase the rate of nucleation into de metallic pool rather than dendritic growth. In this case, the solidification is started with a major content of solid fraction in the samples with WC NPs.

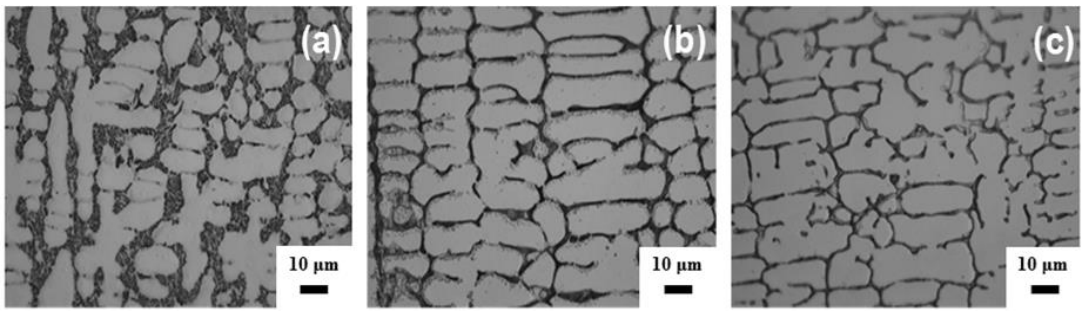

Fig. 2. Optical micrograph of the microstructure of (a) ST1, (b) ST2 and (c) ST3. 1000x.

ISSN 2448-6892

Fig. 3 (a) shows a demarcated area with interdendritic regions with lamellar eutectic phases (I1). Moreover, the Fig. 3 shows a good metallurgy bonding between the substrate and overlays after solidification of the metallic pool without and with 0.5 and 2 wt% of WC NPs. This fact is due to the high thermal gradient and analogous chemical nature, which leads the high diffusing effect in the interface of filler metal and substrate [17]. In the Fig. 3 (b) were observed carbides in the boundary of dendritic (I2) as well as morphology spherical (I3) (Fig. 3 (c)).

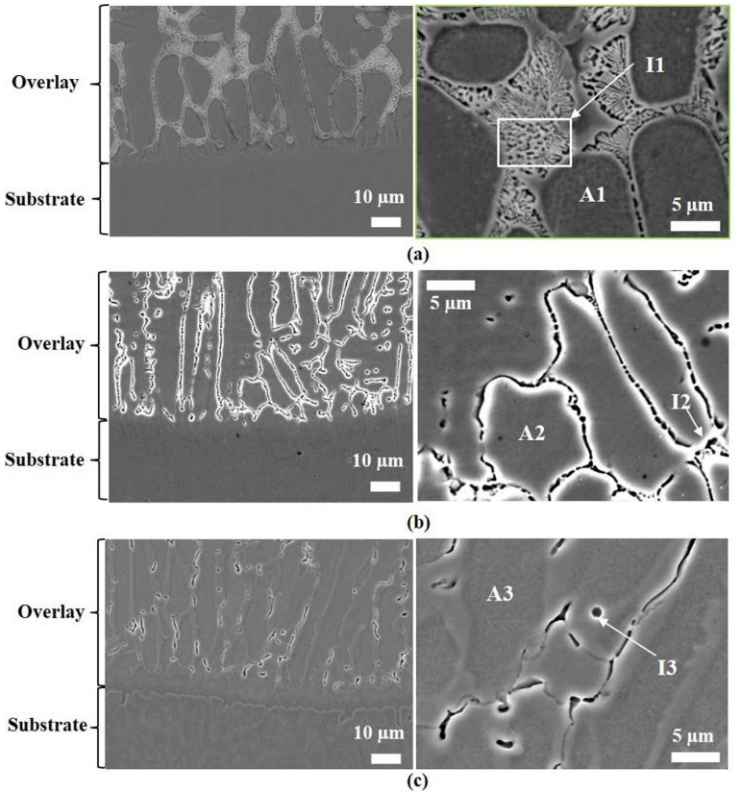

Fig. 3. SEM images of overlay/ substrate interface of ST1 (a), ST2 (b) and ST3 (c).

Table 2 summarizes the elemental chemical composition of the overlays by EDX analysis. According to the Table 2, the dendritic matrix (A1 region) of the unmodified Stellite 12 overlay (ST1) mainly consisted of carbon, chromium, iron and cobalt with a small amount of silicon, manganese and tungsten. It is noticeable that the addition of WC NPs (ST2 and ST3) to the original alloy (ST1) reduced the interdendritic zone, and the mainly constituents of dendritic matrix (A2 and A3 region) was modified, i.e. an increase on carbon and iron at% and a decrease on chromium, cobalt and tungsten at% was reached. A similar behavior was observed on the interdendritic zone, where the lamellar eutectic (Fig. 3 (a), I1 region) rich on carbon, chromium, iron and cobalt at%, was modified with the addition on WC NPs to become a globular shape, a reduction on the interdendritic zone (I2 and I3 region, Table 2), an increase on carbon and iron

ISSN 2448-6892

at%, and a decrease on chromium, cobalt and tungsten at%. EDX analysis conducted on ST1, ST2 and ST3 revealed that the iron diffused from the substrate to the overlay, while the WC NPs were added, according to the atomic percentages observed in Table 2.

Table 2. EDS analysis of the constituents present in the microstructures of the examined overlays in Fig. 3 (at%).

	A1	A2	A3		I1	I2	I3
C	23.86	27.67	29.35		17.58	11.56	22.93
Si	1.77	1.81	1.51		-	2.2	1.11
S	-	0.3	0.36		0.71	0.8	0.6
Cr	14.66	11.07	8.98		17.38	12.52	11.6
Mn	0.36	0.36	-		0.48	0.42	0.36
Fe	32.35	42.06	47.83		32.5	51.57	51.32
Co	26.09	16.05	11.32		29.1	19.53	11.48
W	0.91	0.67	0.65		2.26	1.4	0.59

Measurements of microhardness and wear resistance on the overlay.

Since overall, it is accepted that the microhardness of a material is related closely to its resistance to wear and more wear resistant it is [9,18]. In order to correlate the microhardness with the wear resistance and compare the effect of WC NPs in the overlay, in this work 10 indentations (Fig. 4 (b)) were made along three regions (overlay, HAZ and substrate) in the samples ST1, ST2 and ST3, and then the pin-on-disk test was carried out with a load 5N.

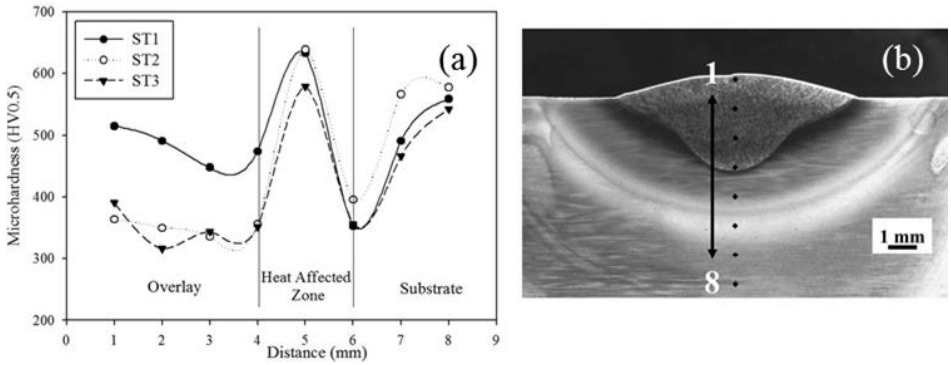

Fig. 4. Microhardness profile (a) and microhardness indentations across the sample (b).

The microhardness behavior analyzed through the three regions in each sample (ST1, ST2 and ST3) are similar. However the impregnation of WC NPs to the cobalt-based Stellite 12 alloy reduced the microhardness of the overlay (Fig. 4 (a)). These microhardness results are directly related to the effect on the inter-dendritic spacing. This result is consistent with the information analyzed that shows the reduction of the carbide formation that consequently reduce the overlay microhardness.

ISSN 2448-6892

Wear test results are presented as volume loss in Fig. 5. The weight loss was converted to the volume loss using the material density, and then was normalized by the load and sliding distance. It is shown that the better result in weight loss was obtained in ST2, followed by ST1 and ST3 respectively, in this graph is remarkable the effect of WC NPs, with an increase in wear resistance, but when the addition of WC NPs is increased to 2 wt%, the wear resistance decreases, which results in greater volume loss. The wear rate was the same behavior of the volume loss, where ST2 exhibited the highest wear resistance with a low wear rate about 4.5 x 10^{-6} mm^3/Nm with 5N load.

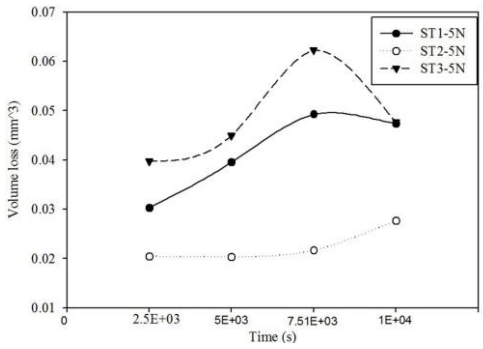

Fig. 5. Pin-on-disk wear test results, volume loss at 5N load.

Conclusions

The interdendritic regions is modified and refinement by the incorporation of WC NPs. It is remarkable that an increase in the weight percentage of WC NPs the interdendritic regions are reduced. Due to that the solidification starts with a major liquid fraction with major nucleation sites.

The interdendritic regions contain a higher content of lamellar eutectic phases that the samples without WC NPs. Likewise, all samples without and with WC NPs have a good metallurgy bonding between the substrate and overlay.

The wear resistance is better in the sample with 0.5 wt% of WC NPs than the samples with more content of nanoparticles. It is postulate that small precipitates are dissolved into metallic pool. In consequence, these solidified precipitates into matrix can interact with dislocations that are generated by the friction so, increase the wear resistance. Besides, this samples content a minor interdendritic region without eutectic phases. So, currently the authors are working with other techniques in order to elucidate the role of the precipitates after wear test and to propose a correlation with the sizes of precipitates and wear. Otherwise, to propose an alternative route to increase the wear and corrosion resistance by the incorporation of WC NPs (wt%).

ISSN 2448-6892

References

1. K. Antony, A. Antony, K. Bhansali, R. Messler, A. Miller and M. Price. *Hardfacing. ASM Handbook*. Vol. 6; 1983. p. 771.

2. D. Chen, D. Liu, Y. Liu, H. Wang and Z. Huang. "Microstructure and fretting wear resistance of ɣ/TiC composite coating in situ fabricated by plasma transferred arc cladding". *Surf Coat Technol*; 239 (2014) 28-33.

3. J. Shin, J. Doh, J. Yoon, D. Lee and J. Kim. "Effect of molybdenum on the microstructure and wear resistance of cobalt-base Stellite hardfacing alloys". *Surf Coat Technol*; 166 (2003) 117-126.

4. A. Neville and T. Hodgkiess. "Characterisation of high-grade alloy behaviour in severe erosion–corrosion conditions". *Wear*; 233-235 (1999) 596-607.

5. P. Crook. Properties and Selection: Nonferrous Alloys and Special-Purpose Materials. *Metals Handbook*. 10th ed., vol. 2; 1993, p. 446.

6. J. Davis. Nickel, cobalt, and their alloys. Materials Park (OH): *ASM International*; 2000.

7. W. Betteridge. *Cobalt and its alloys*. Chichester: Halsted Press; 1982.

8. Y. Birol. "Thermal fatigue testing of Stellite 6-coated hot work tool steel". *Materials Science and Engineering A*; 527 (2010) 6091-6097.

9. K. Alireza, L. Rong, L. Ming and Y. Qi. "Wear resistant carbon fiber reinforced Stellite alloy composites". *Materials and design*; 56 (2014) 487-494.

10. P. Mendez, N. Barnes, K. Bell, S. Borle, S. Gajapathi, S. Guest, H. Izadi, A. Kamyabi and G. Wood. "Welding processes for wear resistant overlays". *Journal of Manufacturing Processes*; 16 (2014) 4-25.

11. P. Huang, R. Liu, X. Wu and M. Yao. "Effects of Molybdenum Content and Heat Treatment on Mechanical and Tribological Properties of a Low-Carbon Stellite® Alloy". *Journal of Engineering Materials and Technology*; 129 (2006) 523-529.

12. W. P, H. Evans and C. Ponton. "Investigation into the wear behaviour of Stellite 6 during rotation as an unlubricated bearing at 600 °C". *Tribology International*; 44 (2011) 1589-1597.

13. H. Yu, R. Ahmed and H. de Villiers Lovelock. "A Comparison of the Tribo-Mechanical Properties of a Wear Resistant Cobalt-Based Alloy Produced by Different Manufacturing Processes". *Journal of Tribology*; 129 (2007) 586-594.

14. A. Motallebzadeh, E. Atar and H. Cimenoglu. "Sliding wear characteristics of molybdenum containing Stellite 12 coating at elevated temperatures". *Tribology International*; 91 (2015) 40-47.

15. G. E. Dieter. Mechanical Metallurgy. Mc Graw Hill. London; 1988, p. 217-218.

16. S. Atamert and H. Bhadeshia. *Metall. Trans*. vol. 20A; p. 1037.

17. Q. Hou, J. Gao and F. Zhou. "Microstructure and wear characteristics of cobalt-based alloy deposited by plasma transferred arc weld surfacing". *Surface & Coatings Technology*; 194 (2005) 238– 243.

18. I. Konyashin, B. Ries, D. Hlawatschek, Y. Zhuk, A. Mazilkin, B. Straumal, F. Dorn and D. Park. "Wear-resistance and hardness: Are they directly related for nanostructured hard materials?". *Int. Journal of Refractory Metals and Hard Materials*; 49 (2015) 203–211.

ISSN 2448-6892